

Nano Lett. Author manuscript; available in PMC 2007 April 20.

Published in final edited form as: *Nano Lett.* 2005 August; 5(8): 1563–1567.

# Visualization of Individual Single-Walled Carbon Nanotubes by Fluorescent Polymer Wrapping

Vladimir V. Didenko<sup>†</sup>, Valerie C. Moore<sup>‡</sup>, David S. Baskin<sup>§</sup>, and Richard E. Smalley<sup>‡</sup>
Department of Neurosurgery, Baylor College of Medicine, 2002 Holcombe Boulevard, Building 109
Room 204, Houston, Texas 77030, Department of Neurosurgery, The Methodist Neurological
Institute, 6560 Fannin, Suite 944, Houston, Texas 77030, and Department of Chemistry, Rice
Quantum Institute, and Center for Nanoscale Science and Technology, Rice University, Houston,
Texas 77005

# **Abstract**

Manipulating optical properties of single-walled nanotubes (SWNTs) is necessary for the development of nanoscale optical devices and probes for biomedical research. In life sciences it will make possible the direct observation of SWNTs inside living cells using optical microscopes. In the nanotechnology field it will enable the development of nanosensors with fluorescent reporting. However, the direct fluorescent labeling of SWNTs is obstructed by their strong light quenching qualities. Besides, chemical functionalization of SWNTs needed for the covalent attachment of fluorescent dyes could change favorable properties of nanotubes. Here we report that optical properties of SWNTs can be manipulated without their covalent modification by wrapping them with fluorescently labeled polymer poly(vinylpyrrolidone) (PVP-1300). Fluorescent PVP-1300 forms a monomolecular ~2.5 nm thick layer coiling around individual SWNTs and nanotube bundles. PVP casing is fluorescent although it is only several nanometers thick. This makes individual SWNTs observable by a fluorescent microscope. The spare polymer strands left over after wrapping around the relatively shorter nanotubes form junctions between SWNTs tying them together into new configurations, primarily Y- and Ψ-type junctions. The ability to use a single fluorescent polymer strand to fasten nanotubes together can be useful in assembly of nanotube-made devices. In PVPcovered SWNTs multiple fluorophores are attached to each single nanotube making them unique composite fluorophores attractive as parts of biological fluorescent probes and in the development of the new materials in photonics and nanotechnology.

Fluorescent labeling of single-walled nanotubes (SWNTs) was attempted before using both covalent  $^1$  and noncovalent  $^{2,3}$  modifications. However so far both approaches did not produce satisfactory results. Covalent modifications alter the  $\mathrm{sp^2}$ -bonded graphene sidewall and change physical properties of SWNTs. Besides the fluorophores covalently or noncovalently attached to the nanotube surface were quenched due to energy transfer to the nanotube.  $^{1,3}$  On the other hand, the noncovalent attachment using such dyes as long-chain dialkylcarbocyanines resulted in significant buildup on the SWNTs creating bulky structures visible with optical microscopes even without fluorescence.  $^2$  We have achieved fluorescent labeling of SWNTs without these shortcomings by enveloping them into a thin layer of fluorescent poly-(vinylpyrrolidone).

We produced fluorescent poly(vinylpyrrolidone)-1300 (PVP-1300) by conjugating unlabeled polymer with various Alexa dyes, such as: Alexa Fluor 594 (red fluorescence), Alexa Fluor

Correspondence to: Vladimir V. Didenko.

<sup>†</sup>Baylor College of Medicine.

<sup>‡</sup>Rice University.

<sup>§</sup>The Methodist Neurological Institute.

488 (green fluorescence), and Alexa Fluor 350 (blue fluorescence). Attachment of Alexa fluorophores to PVP-1300 was accomplished via the new application of the classical tyramide-horseradish peroxidase reaction<sup>4</sup> (see Methods). In the reaction horseradish peroxidase activates tyramide-fluorophore conjugates generating active tyramide radicals. Addition of PVP to this reaction mix results in fluorescent labeling of poly(vinylpyrrolidone) via attachment of fluorescently labeled tyramides. Fluorescently tagged PVPs had bright red, green, or blue fluorescence depending on the fluorophore attached and showed cationic properties when tested in gel electrophoresis (Figure 1 (wells 1–3). PVPs fluorescing red, green, or blue had similar intensity of fluorescence and identical electrophoretic properties; therefore we used only green fluorescent PVP (Alexa Fluor 488 labeled) for our experiments with nanotubes.

Fluorescent coating of SWNTs was accomplished by mixing the suspension of SWNTs stabilized in 1% sodium dodecyl sulfate (SDS) with various amounts of fluorescent PVP-1300 (PVP-FL). We mixed SWNTs with PVP-FL at different ratios in an attempt to estimate the minimal thickness of the coating, which still produced fluorescence. Various SWNT/PVP-FL mixtures were analyzed in electrophoresis, which allowed separation of fluorescent PVP and PVP-coated SWNTs from unreacted tyramide. We used electrophoresis as a method to strip the PVP coating in a controllable fashion so that only a monomolecular layer of PVP was present and to demonstrate that, even in this case, SWNTs did not quench fluorescence. In preliminary experiments we found that without PVP-FL coating the nanotubes did not enter agarose gels and stayed in the wells. However mixing with PVP allowed them to enter the gel where they migrate toward the cathode inside fluorescent PVP as detected by Raman. We used gel electrophoresis to examine different SWNT/PVP-FL ratios; all of the preparations were made by combining increasing volumes of SDS-stabilized SWNTs with fixed amounts of PVP-FL. We found that the ratios above 0.2% did not produce fluorescent bands (Figure 1 (wells 4–7). Surprisingly our subsequent tests showed that this fluorescence quenching was not caused by the increasing concentrations of SWNTs. Instead, increase in SDS concentration was solely responsible for this effect (Figure 1 (wells 8–11). Higher SDS concentrations changed electrophoretic properties of PVP-FL. We observed a complete reversal of PVP-FL migration pattern and its movement toward the anode at SDS concentration above 0.4%, which corresponded to a PVP/SWNT ratio of 0.2% (Figure 1). We noticed the same effect using unlabeled PVP, which produced a weak blue-green fluorescence when illuminated by a 312 nm wavelength UV light and was observable in agarose gels (Figure 2 (wells 8–12).

We reasoned that chaotropic action of SDS in concentrations exceeding 0.4% disrupted formation of the PVP-FL layer on the surface of nanotubes. Exceedingly long PVP-1300 molecules are very likely to entangle during the wrapping process thus associating more unwrapped polymer for a given surface area coverage. Due to the additional polymer entanglement the formation of more than a monolayer thick polymer coating was possible at high polymer and low SDS concentrations. This additional material, which is only loosely attached to the wrapped nanotubes, nevertheless contributes the most fluorescence at the higher concentrations of PVP-FL because it is positioned at a longer distance from SWNT sidewall. Mild increase in SDS concentration disrupts this loosely attached polymer before affecting the tightly wrapped PVP-FL, which is associated with nanotubes with a much stronger force.

When electric current was applied, the loosely associated PVP-FL migrated in the opposite direction, whereas SWNTs partially stripped of their coating lost a significant amount of positive charge contributed by PVP-FL and were expected to slow and eventually stick in the gel. This was supported by our observation that fluorescent bands containing nanotubes significantly slowed their migration almost to a complete stop after ~30 min of electrophoresis despite continuing electric current. Therefore the thinnest coating of SWNTs still producing fluorescence was present at 0.4% SDS concentration (e.g., 0.2% SWNTs/PVP-FL ratio)

(Figure 1 (well 6)). It was critical to determine how much PVP-FL was still wrapped around SWNTs at these conditions. If in this situation the polymer was forming a tight monolayer, then a conclusion could be made that a monolayer-thick polymer wrapping was producing observable fluorescence.

We performed direct observation and measurements of this minimal fluorescent coating by taking transmission electron microscopy (TEM) images of SWNT/PVP-FL prepared at 0.4% SDS concentration. The images show individual nanotubes and small bundles associated with a monolayer of polymer. We observed two variants of PVP-FL packaging on the surface of individual 0.7-1.1 nm diameter nanotubes: ~2.5 nm thick areas and ~0.7 nm thick areas. The thicker areas were periodically interrupted by the zones with thinner polymer cover (Figure 3A). This is consistent with a notion that the zones with tightly coiled polymer (2.5 nm areas) are followed by the zones with relaxed polymer coiling. Being driven by strong thermodynamic forces, <sup>5</sup> the tense polymer coiling requires very high molecular flexibility. This might create strong internal stress, which has to be relaxed by zones of less tight packaging. In support of this notion we observed no similar relaxed zones in polymer covers of nanotube bundles, which are thicker and do not have the same requirements for polymer flexibility (Figure 3B, Figure 4). The structure of the polymer covering is clearly demonstrated in TEM images of thin bundles. Fluorescent PVP is seen as ~2.5 nm wide strings tightly coiled around bundled SWNTs (Figure 3B, Figure 4). The PVP wrapping is highly orderly similar to the packaging of a wire in an induction coil or a thread on a reel (Figure 4). The 2.5 nm loops of the polymer helix are tightly pressed to each other leaving no uncovered space and resembling a stack of pancakes (Figure 4).

The relationship between the polymer length and configuration of the wrapped nanotubes requires additional analysis. In this work we used PVP-1300, one of the longest of the commercially available PVPs. SWNTs on the other hand were relatively short. We have previously analyzed this type of nanotube for the length distribution, which was determined at  $137 \pm 130$  nm. In this situation a single polymer molecule not only would cover the entire surface area of a single SWNT but also would have a significant part of the strand left unused after wrapping. This excessive strand could react with other uncovered or partially covered SWNTs entangling them with the result of bundling several nanotubes together in Y- and  $\Psi$ -type junctions. This type of entanglement is different from a loose association between polymer molecules, which we discussed before. In the case of nanotubes, the strength of association is much higher as it is thermodynamically driven to eliminate the hydrophobic interface between SWNTs and the aqueous medium and therefore it should not be affected by a mild increase in SDS concentration.

We indeed detected significant amounts of such structures in TEM images. Y-type junctions between individual nanotubes (Figure 3A) and small nanotube bundles (Figure 4B), as well as  $\Psi$ -type junctions between thin bundles (Figure 3B, Figure 4A) were pretty common among polymer-wrapped SWNTs derived from the SDS-stabilized solution where primarily individual SWNTs were present (see Methods). In additional support of this notion we did not detect Y- and  $\Psi$ -type junctions when a shorter PVP-40 was used to wrap SWNTs.  $^5$ 

The diameter of a new thicker bundle, created after two wrapped SWNTs (Figure 3A) or several wrapped bundles (Figure 3B, Figure 4) are joined together, is significantly smaller than the sum of the diameters of the initial parts. In the case of individual SWNTs, the diameters of nanotubes inside polymer casing can be estimated as in the example in Figure 3A where joining of individual wrapped SWNTs with diameters of 5.5 nm + 5.9 nm results in a 6.9 nm bundle. This suggests that the thickness of the polymer cover stays the same in the resulting bundle as its overall thickness is increased solely by the diameter of the additional nanotube. In the discussed example this is consistent with 2.5 nm cover thickness in the resulting bundle

containing a 1.1 nm diameter nanotube (from 5.9 nm branch) and a 0.8 nm diameter nanotube (from 5.5 nm branch) vs 2.4 nm polymer thicknesses in the initial branches. However this does not hold in the case of joining of nanotube bundles, as these bundles can comprise already wrapped SWNTs. One example is presented in Figure 4B, where joining of the two individual wrapped nanotubes ( $d \sim 5.5$  nm) results in a bundle with a diameter  $\sim 16$  nm, which is consistent with an additional 2.5 nm layer of polymer fastening two nanotubes to each other.

The ability to link nanotubes by a new mechanism of tying them together with a long polymer strand, which in itself could be modified to carry various functional species, is potentially useful for the assembly of the nanotube-made devices. Its additional utility, compared to the overall modification of the nanotube wall, is in the reversibility of the connection and in the unique possibility to connect nanotubes at a limited length leaving unbundled parts available for additional modifications.

One of the tasks of this research was to estimate if a thin layer of fluorescently labeled PVP covering nanotubes was sufficient for the prevention of fluorescence quenching. Therefore we directly examined fluorescently labeled SWNTs using a fluorescent microscope. A suspension of SWNTs coated by PVP-FL at the 0.2% ratio (0.4% SDS) was deposited onto a glass surface by a brief centrifugation. Samples were analyzed using light and fluorescence detection. The slide was examined using Olympus IX-70 fluorescent microscope equipped with a Nikon digital video camera under 490 nm excitation light and 520 nm emission light, using an oil immersion objective. We observed individual fluorescent SWNTs and their bundles deposited on the glass (Figure 5). The theoretical resolution limit of any optical system is limited by diffraction and is ~200 nm, whereas the TEM measured width of fluorescing wrapped SWNTs was in a 5–20 nm range. Although Prakash et al. <sup>2</sup> stated that nanotubes with diameters as small as 14 nm could be observed in optical images, in our experience in nonfluorescent format only the thickest bundles of nanotubes, as thick as perhaps 100 nm, could be observed with their apparent diameters perceived as equal to the lower resolution limit (Figure 5B). A multitude of thinner PVP-FL coated nanotubes especially in a 5–15 nm range was unobservable using an optical nonfluorescent system. The situation with fluorescence detection was different. As each fluorophore can be thought of as a light source, much smaller objects and potentially a single fluorescent molecule can be visualized. Therefore when we used fluorescence to examine PVP-FL SWNTs deposited on the glass slide, we detected multiple fluorescent nanotubes, which were too thin to be seen in nonfluorescent images (Figure 5C). Their numbers significantly exceeded that of the thicker nanotube bundles seen in both optical and fluorescent formats (Figure 5A,B). Although similar to TEM images we detected fluorescing Y-junctions among nanotube bundles deposited on glass (Figure 5B), there were practically no junctions among individual fluorescent nanotubes, which all had linear shapes. We therefore concluded that a thin layer of fluorescently labeled PVP covering nanotubes was sufficient for the prevention of fluorescence quenching.

A structure of PVP-FL wrapped nanotubes could play a role in this protective effect. In these polymer-covered SWNTs a positively charged PVP backbone is sandwiched between a negatively charged nanotube surface and a negative layer of Alexa Fluor residues. This minimizes interactions between fluorophores and the nanotube surface preventing fluorescence quenching.

On the basis of our results we conclude that SWNTs could be fluorescently labeled via noncovalent coating with a fluorescent polymer. Such nanotubes have a potential to serve as unique fluorescent probes because multiple fluorophores attached to the surface of a single nanotube make it a convenient composite fluorophore applicable for detection of single molecule events. In addition to fluorophores a plethora of other organic molecules such as proteins, antibodies, or DNA can be easily conjugated to PVP and used to cover SWNTs.

#### Methods

# Fluorescent Labeling of PVP Using Tyramide and Peroxidase

Fluorescent labeling was performed in 50 mM Tris-HCl, pH 8.0, containing  $20 \,\mu\text{g}/\mu\text{L}$  PVP-1300,  $200 \,\text{ng}/\mu\text{L}$  horseradish peroxidase, 0.01% hydrogen peroxide, and 1:50 dilution of tyramide-Alexa Fluor 488 stock solution (from catalog no. T-20932) (Molecular Probes) (or Alexa Fluor 350 or Alexa Fluor 594) for 1 h at 37 °C.

# **SWNTs**

SWNTs were purified by wet air oxidation followed by a HCl wash.<sup>6</sup> Purified SWNTs were suspended in water with SDS through a process of homogenization, sonication, and centrifugation.<sup>7</sup>

# **PVP Coating of SWNTs**

SWNTs were coated with PVP by mixing various volumes of SWNT suspension (15  $\mu$ g/ mL) stabilized in 1% SDS with a solution of 130 kDa poly-(vinylpyrrolidone) (PVP-1300) in water. We used 0.005%, 0.01%, 0.05%, 0.1%, 0.15%, 0.2%, 0.3%, and 0.4% ratios of SWNTs/PVP.

### **Gel Electrophoresis**

Small aliquots of labeling mix containing fluorescent PVP-coated SWNTs were loaded in 3% ficoll on 1% agarose gel in 1xTBE, and run for 1 h at 100 V/mA. They were observed using an FBTIV-88 transilluminator (Fisher Scientific) ( $\lambda$  = 312 nm). Gel images were captured by a PC1015 Canon digital photo camera equipped with a 4-megapixel CCD and processed in Adobe Photoshop 7.0.

## Raman Analysis

Raman was performed on a Kaiser Optical Systems, Inc., Raman Rxn System with a 785 nm laser.

#### Transmission Electron Microscopy

TEM was performed on a Hitachi H-7500 transmission electron microscope equipped with Gatan  $2K \times 2K$  CCD using Formvar-coated copper grids. Distances were estimated electronically at the time of image acquisition.

## References

- 1. Zhu W, Minami N, Kazaoui S, Kim Y. J Mater Chem 2003;13:2196.
- 2. Prakash R, Washburn S, Superfine R, Cheney RE, Falvo MR. Appl Phys Lett 2003;83:1219.
- 3. Riggs JE, Guo Z, Carroll DL, Sun YP. J Am Chem 2000;122:5879.
- 4. Gross AJ, Sizer IW. J Biol Chem 1959;34:1611. [PubMed: 13654426]
- 5. O'Connell MJ, Boul P, Ericson LM, et al. Chem Phys Lett 2001;342:265.
- Chiang IW, Brinson BE, Huang AY, Willis PA, Bronikowski MJ, Margrave JL, Smalley RE, Hauge RH. J Phys Chem B 2001;105:8297–8301.
- 7. O'Connell MJ, Bachilo SM, Huffman CB, Moore VC, et al. Science 2002;297:593. [PubMed: 12142535]

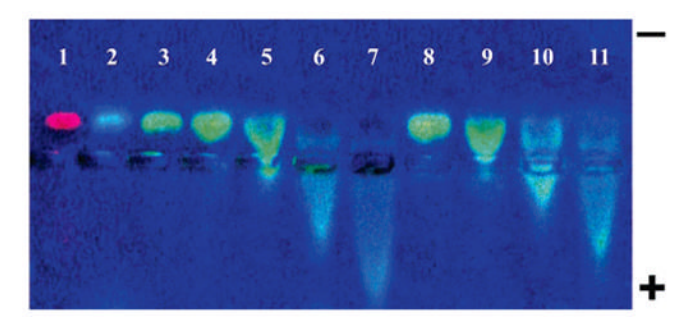


Figure 1. Effects of increasing SDS concentrations on gel electrophoresis of fluorescently labeled PVP-1300 and PVP-1300-coated SWNTs. Wells 1–3 PVP labeled with Alexa Fluor 594 (red fluorescence), Alexa Fluor 350 (blue fluorescence), and Alexa Fluor 488 (green fluorescence). Wells 4–7 SWNTS coated in green fluorescent PVP: well 4, 0.05% SWNT/PVP ratio (0.1% SDS); well 5, 0.1% SWNT/PVP ratio (0.2% SDS); well 6, 0.2% SWNT/PVP ratio (0.4% SDS); well 7, 0.3% SWNT/PVP ratio (0.7% SDS). Wells 8–11 only fluorescent PVP and SDS no SWNTs: well 8, 0.1% SDS; well 9, 0.2% SDS; well 10, 0.4% SDS; well 11, 0.7% SDS. Amount of PVP in all wells was 35  $\mu$ g/well. Note identical changes in the direction of movement of PVP-FL and PVP-FL SWNTs caused by SDS.



Figure 2. Effects of increasing SDS concentrations on gel electrophoresis of fluorescently labeled and unlabeled PVP-1300: wells 1–5, fluorescently labeled PVP; Wells 8–12, unlabeled PVP (100  $\mu$ g/well) seen because of its intrinsic blue fluorescence. SDS concentrations: wells 1 and 8, 0% SDS; wells 2 and 9, 0.2%; wells 3 and 10, 0.4%; wells 4 and 11, 0.6%; wells 5 and 12, 0.8% SDS. Note the identical changes caused by SDS in labeled and unlabeled PVP.

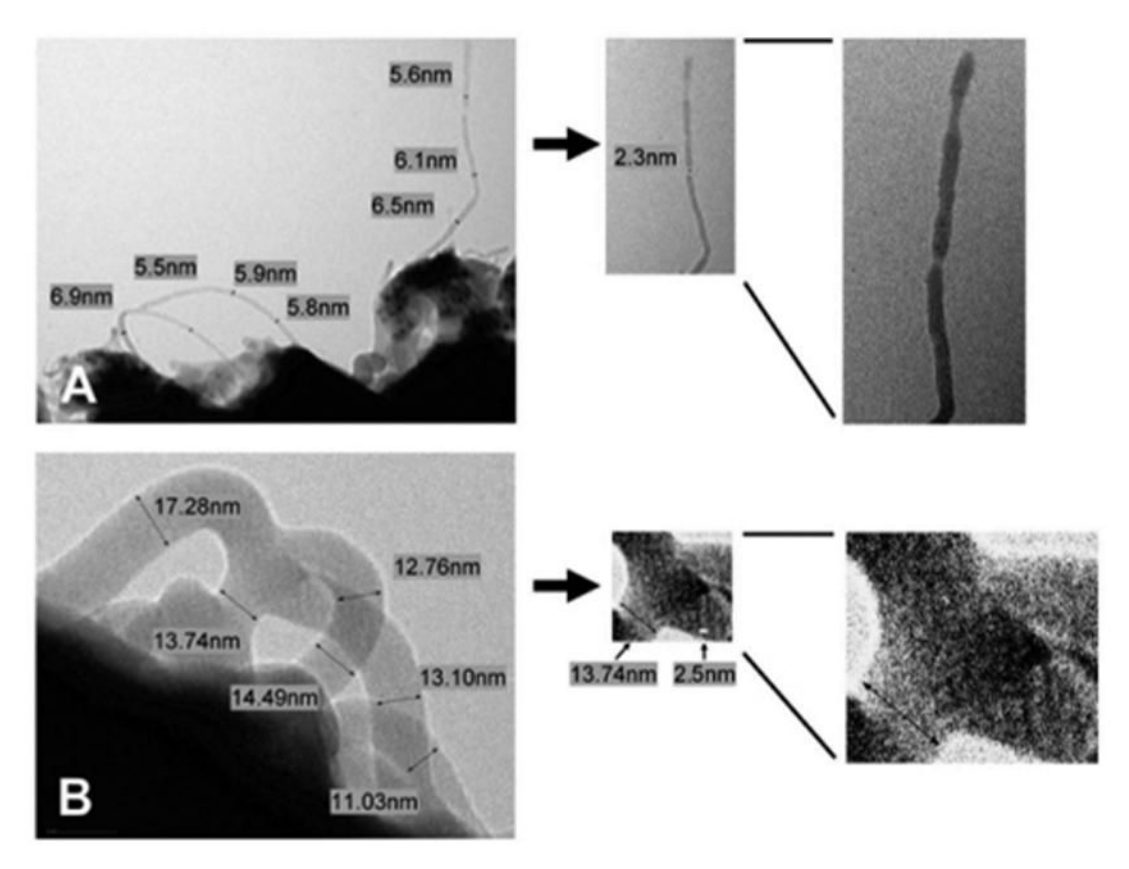


Figure 3. Electron microscopy of PVP-FL-coated SWNTs prepared at 0.2% SWNT/PVP ratio (0.4% SDS). (A) Individual nanotubes ( $d \sim 0.7-1.1$  nm) coated with fluorescently labeled PVP. Note the uneven diameter of coated SWNTs, which on average is close to 6 nm (polymer coat thickness ~2.5 nm) representing zones of tighter coiling of the polymer. Zones with the shorter diameter ~2.3 nm (polymer coat thickness ~0.7 nm) represent areas of relaxed coiling. (B)  $\Psi$ -junction between thin bundles of PVP-FL-coated SWNTs. Expanded part of the image with increased contrast shows PVP-FL strands ( $d \sim 2.5$  nm) tying together thin nanotube bundles.

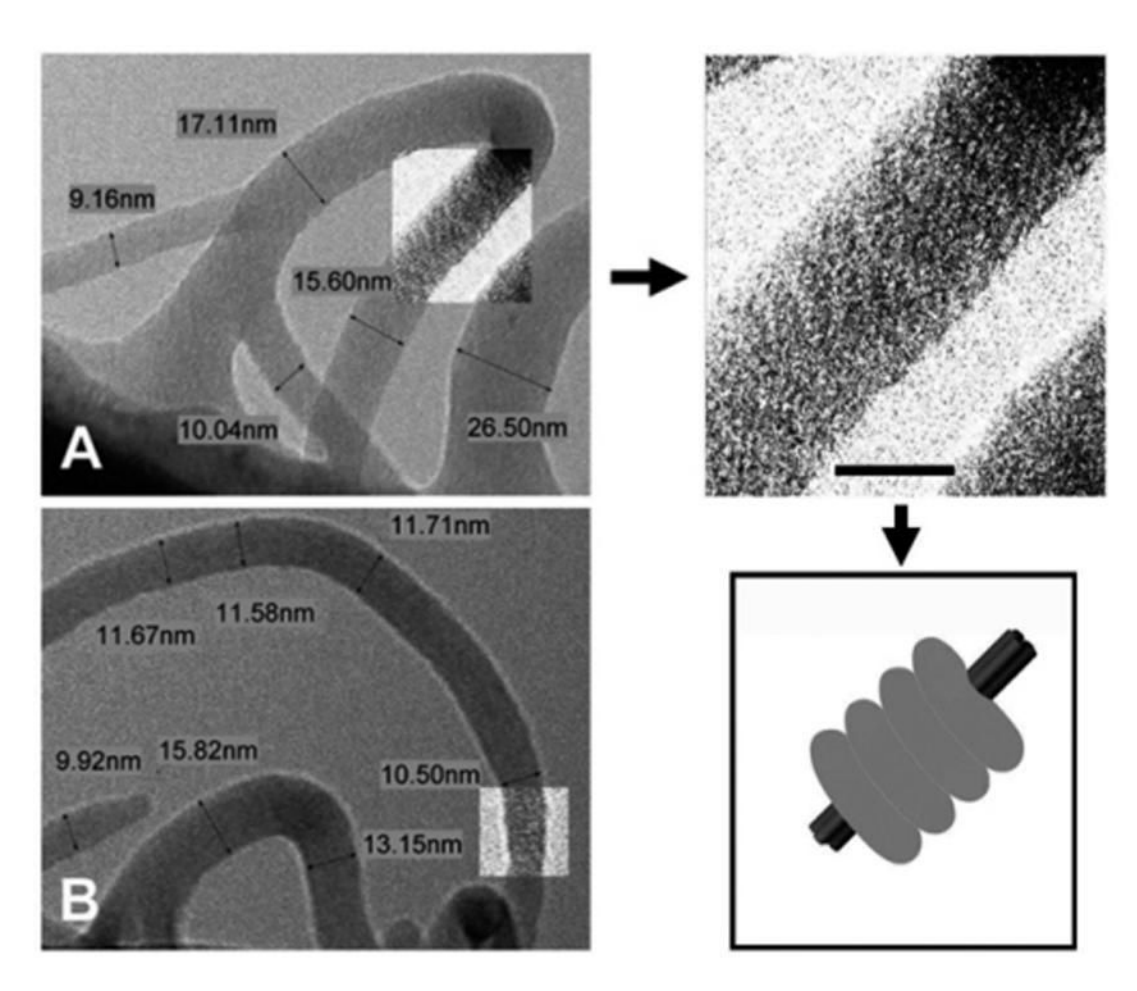


Figure 4. Electron microscopy of fluorescent PVP-coated SWNTs prepared at 0.2% SWNT/PVP ratio (0.4% SDS). (A) A  $\Psi$ -junction between thin bundles of PVP-FL-coated SWNTs. Arrow points to the expanded part of the image with increased contrast. Note tight stacking of the polymer coils. (Bar represents 10 nm.) This wrapping arrangement with tight coiling of PVP-FL around a small bundle of 8, 8 SWNTs is illustrated by the schematic on the right. (B) A Y-junction assembled from two individual coated nanotubes (seen at the lower left corner of the image). Note part of the image with increased contrast showing a "stack of pancakes" polymer coiling.

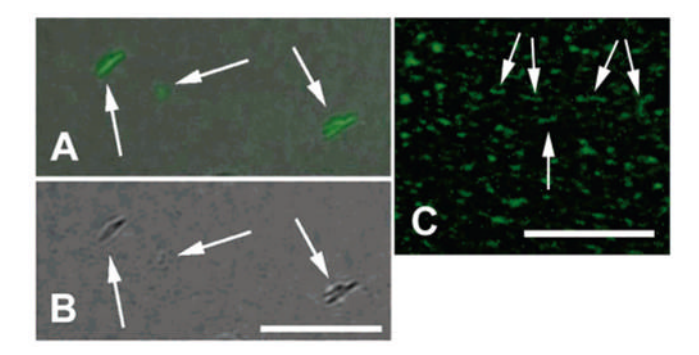


Figure 5. Fluorescing PVP-coated SWNTs deposited on a glass slide. (A) Combined light and fluorescent microscopy of nanotube bundles. Note a Y-junction on the right. (B) Light microscopy of the same bundles. Bar repesents 7  $\mu$ m. (C) Individual fluorescent nanotubes are only seen using fluorescence detection. Note linear fluorescent nanotubes with the absence of junctions. Bar represents  $4\mu$ m.